scientific reports

Check for updates

OPEN

Nonlinear optical and DFT study of natural dye extracted from *Lawsonia inermis* leaves using He–Ne laser

S. Jeyaram[1]✉, A. G. Bharathi Dileepan[2], M. Vishalatchi[2], K. Jayasheela[1], S. Murali[3], Mohammad Ahmad Wadaan[4], Nawaf D. Almoutiri[4], Saheed Olanrewaju Oseni[5] & Madhappan Santhamoorthy[6]

This study presents the third-order nonlinear optical (NLO) properties of a natural dye derived from *lawsonia Inermis*, investigated using Z-scan with continuous-wave He–Ne laser at a wavelength of 632.8 nm. The natural dye exhibited self-defocusing nonlinear refractive index and reverse saturable absorption (RSA) based nonlinear absorption coefficient. The self-defocusing behavior arises from thermal nonlinearity, while the RSA effect is attributed to a higher excited-state absorption cross-section compared to the ground state. The nonlinear refractive index and nonlinear absorption coefficient of the natural dye are determined to be on the order of 10^{-8} cm^2/W and 10^{-3} cm/W, respectively. The natural dye exhibited a substantial third-order NLO susceptibility (χ^3), measured to be on the order of 10^{-7} esu. FT-IR analysis is employed to determine the functional groups present in the natural dye. Density functional theory (DFT) calculations corroborate the experimental findings by providing insights into the NLO properties, molecular electrostatic potential (MEP) and frontier molecular orbit (FMO) of the natural pigments. The results offer valuable insights into the natural dye extracted from *lawsonia Inermis* leaves, highlighting its potential for nonlinear optical applications.

Keywords *Lawsonia inermis* leaves, Third-order NLO, Z-scan, DFT, RSA, Self-defocusing

Significant research has been devoted to nonlinear optical (NLO) materials for photonic technologies, primarily due to their urgent relevance in telecommunications[1,2]. Organic compounds are widely regarded as promising NLO materials[3–5] because they contain delocalized electrons along with D-π-A molecular system that can easily respond to strong electric fields. Among these, many commercial dyes, particularly organic ones have been examined for their NLO features[6–8]. Natural dyes are often favored over synthetic alternatives because they are eco-friendly and cost-effective[9,10]. Unlike synthetic dyes that typically require complex manufacturing processes, natural dyes can be easily extracted from plants, fruits, vegetables, roots, etc. Nature provides a rich variety of dye sources, including leaves, roots, seeds, bark, fruits, vegetables, and flowers, as well as animal and mineral origins[11]. The wide spectrum of natural colours is due to pigments, which are mainly classified into four categories: carotenoids, chlorophylls, betalains, and flavonoids[12]. These pigments possess conjugated structures, absorb visible light, contain chromophores, and exhibit electron resonance, all contributing to the coloration of the dyes[13]. Natural dyes are widely used in colouring textiles, food, cosmetics, and pharmaceuticals[14–17]. In photonic applications, they are increasingly being explored for use in dye lasers, dye-sensitized solar cells (DSSCs), and nonlinear optics[18,19]. Recent years have seen growing interest in assessing the NLO properties of natural dyes for potential use in optical limiters and optical switches[20–23]. However, their adoption remains limited due to inconsistent availability of plant sources and their tendency to degrade faster under light exposure compared to synthetic dyes. Over the years, our research groups have explored various natural pigments, including anthocyanin from *blueberry*[24], β-carotenoid from *Phyllanthus niruri*[25], chlorophylls from

[1]Department of Physics, Takshashila University, Ongur (PO), Tindivanam (TK), Villupuram, Tamilnadu 604305, India. [2]Department of Chemistry, Takshashila University, Ongur (PO), Tindivanam(TK), Villupuram, Tamilnadu 604305, India. [3]Senior Scientific Officer, Nanotechnology Research Centre, SRM Institute of Science and Technology, SRM Nagar, Kattankulathur, Tamilnadu 603203, India. [4] Department of Zoology, College of Science, King Saud University, P.O. Box 2455, 11451 Riyadh, Saudi Arabia. [5]Department of Physics, Lagos State University, Badagry Express Way, P.M.B 0001, LASU Post Office, Ojo, Lagos, Nigeria. [6]School of Chemical Engineering, Yeungnam University, Gyeongsan 38544, Republic of Korea. ✉email: jeyaram.msc@gmail.com

Andrographis paniculata and *Coriandrum sativum* leaves[26,27], lycopene from *tomato*[28], curcumin from *Curcuma longa*[29], betanin from *Beta vulgaris*[30], as well as natural pigments from *Ocimum tenuiflorum* and *Aloe vera*[31,32]. In all NLO studies, a low-power continuous-wave diode laser has been employed to evaluate the nonlinear refractive index, nonlinear absorption coefficient, and third-order NLO susceptibility. The present work focuses on the third-order NLO properties of the natural dye derived from *lawsonia Inermis* using a He–Ne laser.

Materials and methods

Analytical grade ethanol and distilled water are procured from Merck India Ltd. Fresh henna leaves are sourced from the local market, subsequently sun-dried for approximately one week, and then pulverized into a fine powder using a mechanical grinder. The optimized structure of *lawnson* is shown in Fig. 1.

Extraction of natural dye from lawsonia inermis leaves

The Soxhlet experiment technique is employed to isolate natural pigments from henna leaves. A 1000 mL round bottom flask is charged with 500 mL of solvent (60% ethanol in distilled water). Finely powdered henna leaves (10 g) were placed in the thimble of the Soxhlet extractor. The extraction is conducted at 80 °C when using 60% ethanol, and at 110 °C when using distilled water as the solvent. The process is continued until the siphoning solvent in the Soxhlet chamber became nearly colourless, indicating exhaustive extraction. One extraction cycle is defined as the filling of the Soxhlet chamber with solvent followed by its siphoning back into the round bottom flask.

Z-scan method

Z-scan technique consists of a continuous wave (CW) laser working at 632. 8 nm wavelength with total power of 12 mW. The light is focused by a convex lens with focal length of 20 cm. The sample is placed in a cuvette of thickness 1 mm and sweep between −10 mm and +10 mm. The detector is used to measure the output transmittance which is placed at a far-field position. The Rayleigh length of the sample is measured to be 4.7 mm which is greater than the sample length. The schematic experimental setup of Z-scan technique is shown in Fig. 2.

Results and discussion

UV-Visible study

Title compound is used as a dye in the cosmetic industry and ultra-violet-visible spectrophotometry (UV-Vis) used to characterize the dyes extracted from Henna as shown in Fig. 3. The most significant feature of the *lawsone* molecule is its ability to absorb visible light between 500 and 800 nm. The studied dye shows two remarkable peaks. The first around 530 nm and second at 620 nm. These peaks could serve to increase the charge transfer reaction under sun illumination in the final due to oxygen impact. Also, the variation in the UV-Vis absorbance regions reflects the specific phytochemicals present in each plant species[33].

FT-IR study

The vibrational assignments obtained from experimentally are recorded using FT-IR spectra, correlated with theoretically predicted wavenumbers using the density functional method, is presented in Fig. 4. In aromatic compounds, C-H stretching frequencies appear in the range of 3000–3100 cm^{-1}, which are the characteristic area to identify them[34]. The CH stretching modes generally appear in strong intensity regions and are highly polarized. In the title molecule it is observed at 3342 cm^{-1} in FT-IR spectrum. This value has been modifying regular value due to the presence of oxygen element. The C = C stretching vibrations are assigned to carbon

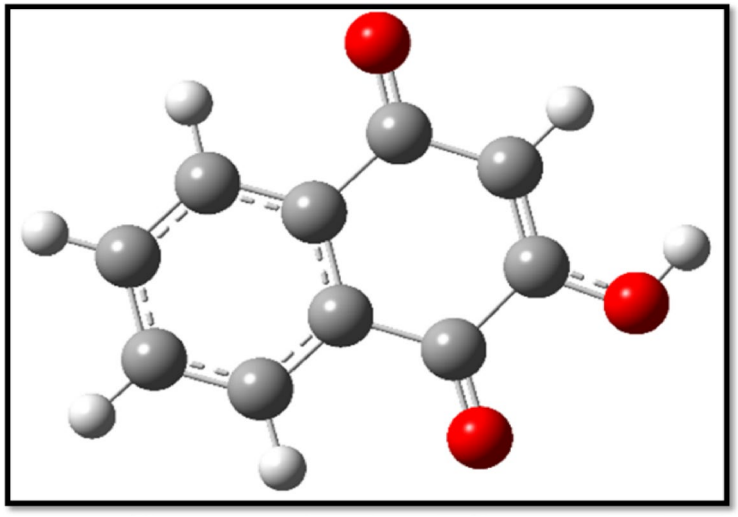

Fig. 1. Optimized structure of *lawson*.

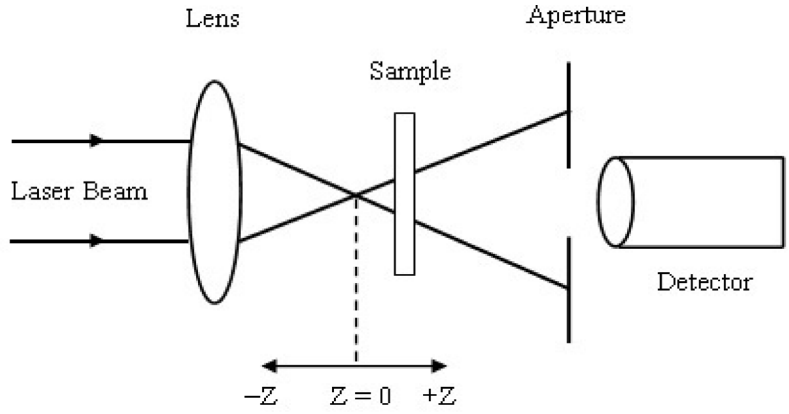

Fig. 2. Schematic experimental setup of Z-scan.

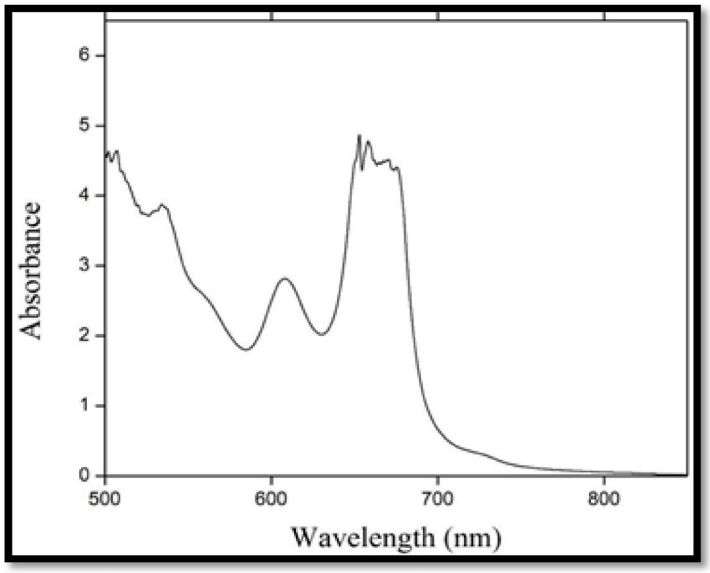

Fig. 3. Experimental UV-visible spectrum.

vibrations in aromatic compounds are in the range of 1400–1650 cm^{-1} [35]. The vibrations are observed at 1653 cm^{-1} experimentally occur in this region. These values are lies in particular region. CO vibrations are in range 1300 –1000 cm^{-1} experimentally occur in 1388, 1155, 1047 cm^{-1}. These values are lies in the expected range.

Third-order NLO study

The third-order NLO features of the natural dye extracted from *lawsonia Inermis* leaves are obtained using the closed aperture (CA) and open aperture (OA) techniques, used to assess the nonlinear refractive index and nonlinear absorption coefficient, respectively. The real and imaginary components of the sample's third-order NLO susceptibility are directly derived from its nonlinear refractive index and nonlinear absorption, respectively. A convex lens is employed to gather the whole transmitted beam during the measurement of the nonlinear absorption coefficient. During the scanning, the position of the sample at -Z and + Z, the transmittance are minimum and gradually increases or decreases at the focus. Figure 5 depicts the OA result of natural dye extracted from *lawsonia Inermis* leaves. The transmittance at the focuses becomes minimum, which means that the sample effectively absorb more light beam at the focus. The deep valley observed at the focus is the result of RSA. The results of RSA is owing to the sample exhibited higher excited state absorption cross-section than the ground state absorption cross-Sect[27]. Under CW laser excitation, induced thermal effects can increase ESA[27], suggesting that ESA-assisted RSA is the NLO mechanism responsible for the observed nonlinearity in the sample. The transmittance in an OA profile can be determined by

$$T(z, s = 1) = \sum_{m=0}^{\infty} \frac{[-q_o(z)]^m}{[m+1]^{\frac{3}{2}}}, for\ |q_o(0)| \quad (1)$$

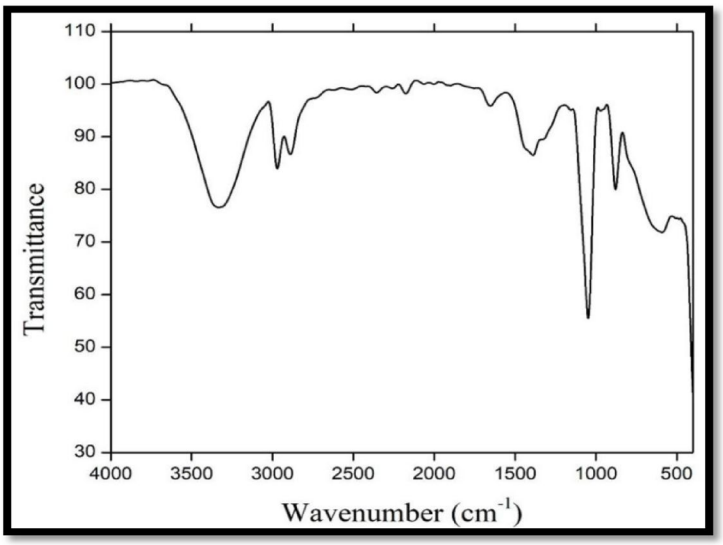

Fig. 4. Experimental FT-IR Spectrum of natural dye.

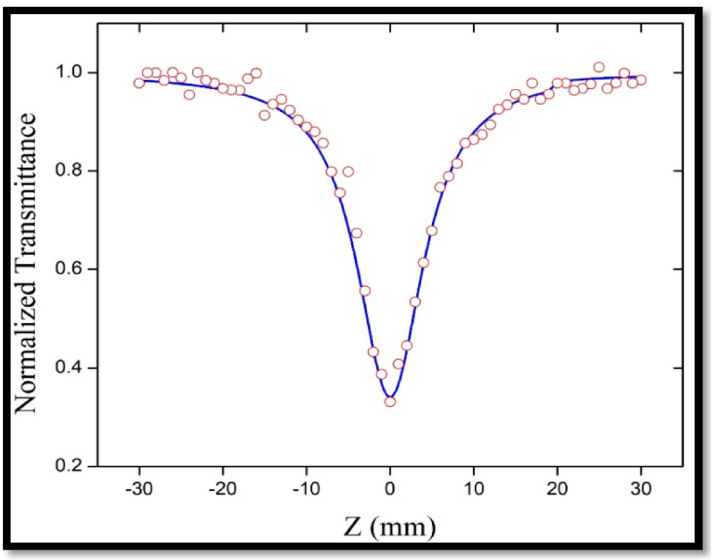

Fig. 5. OA Z-scan result of natural dye extracted from Henna leaves.

where

$$q_0 = \frac{\beta I_o L_{eff}}{\left(1 + Z^2 \Big/ Z_0^2\right)}. \tag{2}$$

The NLO coefficient of absorption (β) of natural dye extracted from *lawsonia Inermis* leaves is given by,

$$\beta = \frac{2\sqrt{2}\Delta T}{I_0 L_{eff}} \left(\frac{cm}{W}\right) \tag{3}$$

where, I_o is the intensity of the beam at focus, L_{eff} is the effective thickness of the sample, Z_o is the diffraction length and Z is the sample position. The values of β of natural dye lawsonia *Inermis* is measured as 3.21×10^{-3} cm/W.

The CA Z-scan technique is used to determine the n_2 of the sample, which directly corresponds to the real part of the third-order NLO susceptibility. In this method, an aperture with a linear transmittance of S = 0.5 is employed. However, the n_2 value obtained from the CA technique does not represent a purely nonlinear

refractive index, as it also includes the contributions from nonlinear absorption. To separate the absorption effects from the refraction component, a simple division method is applied. Figure 6 presents the CA Z-scan results of the sample. The observed peak–valley transmittance profile in Fig. 6 indicates a self-defocusing effect, with thermal effects being the dominant contributing factor. Various NLO mechanisms including electronic, electrostatic and free carrier are involved, in which thermal nonlinearity is most predominant. Continuous absorption of the incident light by the sample leads to a rise in its internal temperature, which in turn alters the refractive index. This refractive index change causes the light to undergo self-defocusing within the medium.

The nonlinear refractive index of natural dye extracted from *lawsonia Inermis* leaves is given by,

$$n_2 = \frac{\Delta \varnothing_0 \lambda}{2\pi I_0 L_{eff}} \left(\frac{m^2}{W}\right) \tag{4}$$

The calculated value of n_2 is -6.68×10^{-8} cm^2/W. The real and imaginary component of third-order NLO susceptibility are measured from n_2 and β of the sample, which is given by,

$$Re\left[\chi^{(3)}\right](esu) = \frac{\epsilon_0 c^2 n_0^2}{10^4 \pi} n_2 \left(\frac{cm^2}{W}\right) \tag{5}$$

$$Im\left[\chi^{(3)}\right](esu) = \frac{\epsilon_0 c^2 n_0^2 \lambda}{10^2 4\pi^2} \beta \left(\frac{cm}{W}\right) \tag{6}$$

Here, ϵ_0 denotes the vacuum permeability, c is the light velocity at vacuum and n_o represents the linear refractive index. The measured values of $Re\left[\chi^{(3)}\right]$ and $Im\left[\chi^{(3)}\right]$ are -2.26×10^{-7} esu and 0.55×10^{-7} esu, respectively. The third-order NLO susceptibility (χ^3) of natural dye extracted from *lawsonia Inermis* leaves is expressed as,

$$\chi^{(3)} = \sqrt{(Re(\chi^3)^2 + (Im(\chi^3)^2}\ (esu) \tag{7}$$

The value of third-order NLO susceptibility (χ^3) of natural dye extracted from *lawsonia Inermis* leaves is 2.32×10^{-7} esu. The second-order polarizability of the natural dye is measured to be 1.40×10^{-31} esu. The experimental findings show good agreement with the theoretical DFT results discussed in the subsequent sections.

Frontier molecular orbit (FMO)

The Homo and Lumo of the title compound is shown in the Fig. 7. HOMO (0.3825) energy is associated with the energy of electron donating ability of a compound, while LUMO (0.0677) energy with electron accepting. The FMO energy gap supplies information about chemical having reactivity with kinetic stability. The frontier orbital energy gap of the title compound is found to be 0.3143 eV. This compound derivative is expected to be less polarizable and associated due to large molecular band gap.

NLO properties

The electric dipole moment, linear polarizability and the hyperpolarizability tensors are explore the NLO properties at the B3LYP/6-311 + + G(d, p) level. The relevance of polarizability and hyperpolarizability of a

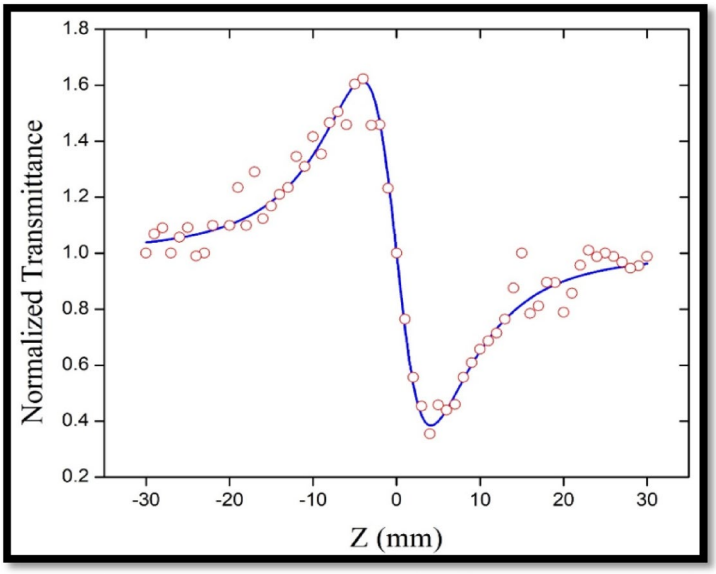

Fig. 6. CA Z-scan result of natural dye extracted from Henna leaves.

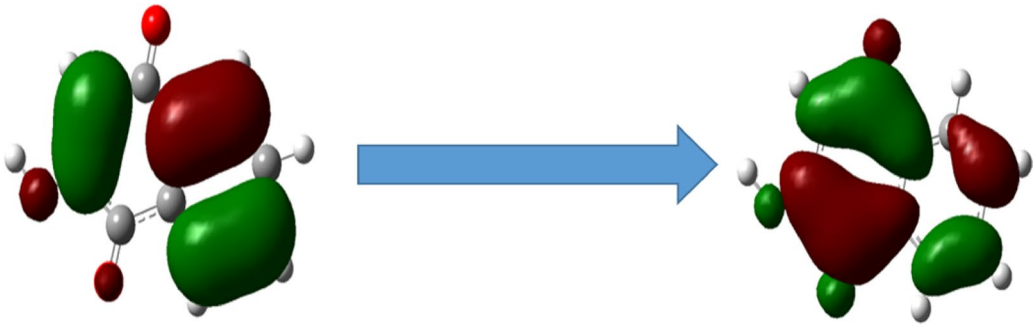

Fig. 7. HOMO-LUMO analysis of the natural dye extracted from *lawsonia inermis* leaves.

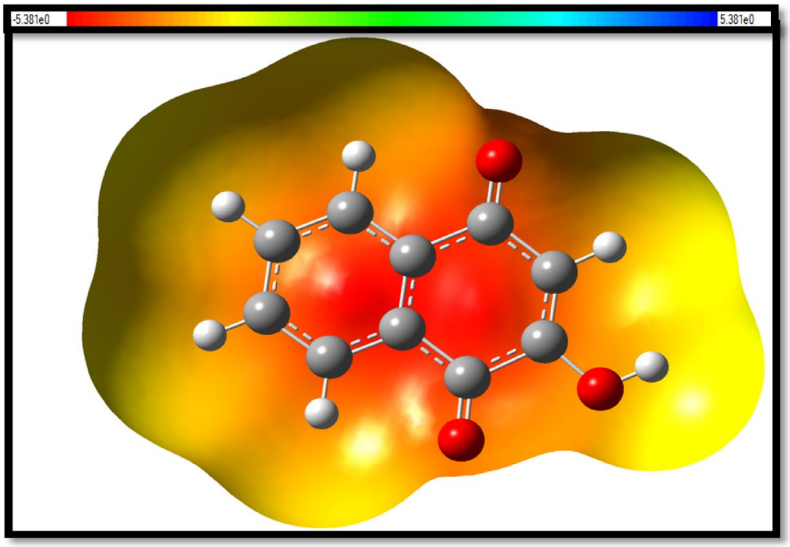

Fig. 8. Molecular electrostatic potential analysis.

molecular system depends on electronic communication between two distinct, which should cause microscopic quadratic and cubic hyperpolarizability with resulting non-zero values derived by the second numerical derivatives of electronic dipole moments to the field implemented[36]. Although dipole moment in this molecules range 0.659×10^{-23} eV, the linear polarizability tensor is highest value is 1.46×10^{-23} eV. It quantifies how the electron distribution within the material can be distorted or shifted when subjected to an external electrical field. The high heperpolarizability values 5.02×10^{-23} eV presented by title compound is indicative that the material shows strong NLO effects. This is crucial for advanced NLO application, such as all optical signal processing, optical switching and the development of highly efficient NLO devices.

Molecular electrostatic potential (MEP)

The molecular electrical potential surfaces illustrate the charge distributions of molecules three dimensionally. This map allows us to visualize variably charged regions of a molecule. Knowledge of the charge distributions can be used to determine how molecules interact with one another and it is also used to determine the nature of the chemical bond. Molecular electrostatic potential is calculated at the B3LYP/6-311 + G (d, p) optimized geometry. There is a great deal of intermediary potential energy, the non-red or blue regions indicate that the electro negativity difference is not very great. In a molecule with a great electro negativity difference, charge is very polarized, and there are significant differences in electron density in different regions of the molecule[37]. This great electro negativity difference leads to regions that are almost entirely red and almost entirely blue. Greater regions of intermediary potential, yellow and green, and smaller or no regions of extreme potential, red and blue, are key indicators of a smaller electronegativity. The color code of these maps is in the range between − 5.381 a.u. (deepest red) to 5.381 a.u. (deepest blue) in compound. The positive (blue) regions of MEP are related to electrophilic reactivity and the negative (green) regions to nucleophilic reactivity shown in Fig. 8. As can be seen from the MEP map of the title molecule, the negative regions are mainly localized on the oxygen atoms. A maximum positive region is localized on the carbon and nitrogen atoms indicating a possible site for nucleophilic attack. The MEP map shows that the negative potential sites are on electronegative atoms (O atom)

as well as the positive potential sites are around the carbon and nitrogen atoms. From these results, it is clear that the carbon and O atom indicates the strongest repulsion.

Conclusion

The third-order NLO parameters of the natural dye extracted from *lawsonia Inermis* leaves were investigated using a CW He–Ne laser operating at a wavelength of 632.8 nm. The Z-scan technique was employed to determine the n_2 and β of the sample. Both CA and OA measurements were conducted, revealing a large nonlinear refractive index on the order of 10^{-7} cm²/W and a significant nonlinear absorption coefficient on the order of 10^{-3} cm/W. The functional groups present in the sample were identified through FT-IR spectroscopy. The real and imaginary components of the third-order NLO susceptibility of natural dye extracted from *lawsonia Inermis* leaves were found to be -2.26×10^{-7} esu and 0.55×10^{-7} esu, respectively. The third-order NLO susceptibility was calculated to be 2.32×10^{-7} esu. The DFT studies supported the experimental results and provided the insightful comment on NLO properties, MEP, FOM. In future research, the dye will be investigated for its optical limiting properties aimed at eye and sensor protection and optical switching device applications. The experimental results demonstrate that natural dye extracted from *lawsonia Inermis* leaves possesses remarkable third-order NLO properties, highlighting its potential for advanced applications in photonics and optoelectronics.

Data availability

The datasets used and/or analysed during the current study available from the corresponding author on reasonable request.

Received: 22 September 2025; Accepted: 11 December 2025
Published online: 20 December 2025

References

1. Latha, N., Sudha, S. & Ramarajan, D. Barathi Diravidamani, structural, spectral,optical and Z-scan budding studies of (E)-N′-(4-bromobenzylidene)fluorobenzohydrazide. *Optik* **247**, 167869 (2021).
2. Subashini, A. et al. Synthesis, growth and characterization of benzylideneaniline compounds: N-(4-bromobenzylidene)-4-fluoroaniline and N-(4- bromobenzylidene)-4-methoxyaniline. *Opt. Mater.* **117**, 111081 (2021).
3. Cai, Z., Zhou, M. & Gao, J. A new type of organic donor-π- acceptorcompounds with third-order nonlinear optical properties. *Opt. Mater.* **31**, 1128–1133 (2009).
4. Chen, J. Q. et al. Nonlinear optical properties of covalent organic frameworks based on completely conjugated donor–acceptor structures. *J. Mol. Liq.* **430**, 127561 (2025).
5. Anusha, B. & Jeyaram, S. Solvatochromism effect on third-order NLO properties of Azo dye. *J. Opt.* **53**, 574–581 (2024).
6. Natarajan Arumugam, A. I. et al. Polar protic and Aprotic solvents induced nonlinear optical and optical limiting properties of Xanthene dye: A DFT study. *Chem. Phys. Imp.* **11**, 100927 (2025).
7. Pengbo Han, D. et al. Third-order nonlinear optical properties of cyanine dyes with click chemistry modification. *Dyes Pigm.* **149**, 8–15 (2018).
8. Jeyaram, S. & Geethakrishnan, T. Third-order nonlinear optical properties of acid green 25 dye by Z-scan method. *Opt. Laser Technol.* **89**, 179–185 (2017).
9. Mundzir Abdullah, M. S., Aziz, G., Krishnan, F., Ahmad, S. M. & Mohammad Ibrahim Abdul Razak, Sulaiman Wadi Haru, large third-order optical nonlinear susceptibility in natural dye derived from clitoria Ternatea petal. *Optik* **256**, 168752 (2022).
10. Lekshmi Jayamohan, J., Kawya, T. C., Sabari Girisun, R. & Muralimanohar Vijayakumar Sadasivan, Nair, nonlinear optical and photostability studies of Allamanda cathartica extract dye. *Opt. Mater.* **148**, 114843 (2024).
11. Zongo, S. et al. Nonlinear optical properties of natural laccaic acid dye studied using Z-scan technique. *Opt. Mater.* **46**, 270–275 (2015).
12. Susmita Ghosh, T., Sarkar, A., Das, R. & Chakraborty Natural colorants from plant pigments and their encapsulation: An emerging window for the food industry. *LWT Food Sci. Technol.* **153**, 112527 (2022).
13. Masyita, A. et al. Natural pigments: innovative extraction technologies and their potential application in health and food industries. *Front. Pharmacol.* **15**, 1507108 (2025).
14. Alegbe, E. O. Taofik Olatunde Uthman, a review of history, properties, classification, applications and challenges of natural and synthetic dyes. *Heliyon* **10**, e33646 (2024).
15. Maryam Sundhu, M. K., Khosa, S., Adeel, T. & Ahamed microwave-assisted eco-friendly acid dyeing of proteinous fabrics using acid violet 3B dye. *J. Nat. Fibers.* **19**, 8065–8074 (2022).
16. Shabbir, M. U. et al. Eco-friendly acid dyeing of silk and wool fabrics using acid Violet 49 dye. *Environ. Sci. Pollut Res.* **30**, 9808–9819 (2022).
17. Batool, F., Adeel, S., Azeem, M. & Iqbal, N. Natural dye color strengthening potential and compounds of selected vegetable residues belonging to brassicaceae: An approach towards sustainability. *Pak J. Bot.* **54**, 29–336 (2022).
18. Geetam Richhariya, A., Kumar, P., Tekasakul, B. & Gupta Natural dyes for dye sensitized solar cell: A review, renew. *Sustain. Energy Rev.* **69**, 705–718 (2017).
19. Kouissa, B. et al. Investigation study on the nonlinear optical properties of natural dyes: Chlorophyll *a* and *b*. *Opt. Commun.* **293**, 75–79 (2013).
20. Prabhakaran, P. K., Suresh, M. X. & Payal, R. S. Saturable absorption, optical limiting and ultrafast laser-induced two-photon fluorescence in *Caesalpinia Sappan* (sappanwood) natural dye. *Opt. Mater.* **162**, 116886 (2025).
21. Das, B. C., Reji, N. & Philip, R. Optical limiting behavior of the natural dye extract from *Indigofera tinctoria* leaves. *Opt. Mater.* **114**, 110925 (2021).
22. Hassan, A. N., Haddad, M. A., Behjat, A. & Golestanifar, M. Optical nonlinearity and all-optical switching in pumpkin seed oil based on the spatial cross-phase modulation (SXPM) technique. *Sci. Rep.* **14**, 18154 (2024).
23. Aparna Thankappan, S., Thomas, V. P. N. & Nampoori Solvent effect on the third order optical nonlinearity and optical limiting ability of betanin natural dye extracted from red beet root. *Opt. Mater.* **35**, 2332–2337 (2013).
24. Sivanukkalai Jeyaram, T. & Geethakrishnan Vibrational spectroscopic, linear and nonlinear optical characteristics of anthocyanin extracted from blueberry. *Res. Phys.* **1**, 100010 (2020).
25. Jeyaram, S. Spectral, third-order nonlinear optical and optical switching behavior of β-carotenoid extracted from phyllanthus Niruri. *Ind. J. Phys.* **96**, 1655–1661 (2022).
26. Jeyaram, S. & Geethakrishnan, T. Linear and nonlinear optical properties of chlorophyll-a extracted from andrographis paniculata leaves. *Opt. Laser Technol.* **116**, 31–36 (2019).

27. Jeyaram, S. & Geethakrishnan, T. Spectral and third-order nonlinear optical characteristics of natural pigment extracted from coriandrum sativum. *Opt. Mater.* **107**, 110148 (2020).
28. Numan, N. et al. On the remarkable nonlinear optical properties of natural tomato lycopene. *Sci. Rep.* **12**, 9078 (2022).
29. Deepa, S. et al. Extraction of natural pigment curcumin from curcuma longa: Spectral, DFT, Third-order nonlinear optical and optical limiting study. *J. Fluoresc*. **34**, 1885–1892 (2024).
30. Sujitha, S. D. A. & Jeyaram, S. Microwave-assisted extraction of betanin from beta vulgaris and their characterization and applications to nonlinear optics. *Ind. J. Phys.* **98**, 1843–1848 (2024).
31. Jeyaram, S., Jeancy, D. & Rany Extraction of natural pigment from ocimum tenuiflorum using different polar solvents and their nonlinear optical characteristics. *J. Fluoresc*. **33**, 287–295 (2023).
32. Jeyaram, S. Natural pigments of Aloe vera: A Third-Order NLO material. *Braz J. Phys.* **52**, 24 (2022).
33. Dorina Simona Codruta Aurora cobzac, Lleana Maria simion, feasibility of UV-Vis spectroscopy combined with pattern recognition techniques to authenticate the medicinal plant material from different geographical areas. *J. Anal. Chem. Technol.* **15**, 17 (2024).
34. Saif Saadaoui, M. A. B. et al. Performance of natural-dye-sensitized solar cells by ZnO Nanorod and nanowall enhanced photoelectrodes. *Beilstein J. Nanotechnol.* **8**, 287–295 (2017).
35. Ahmed Fadlelmoula, O. & Catarino Gcatarino, Graca Minas, Fourier Transform Infrared (FTIR) spectroscopy to analyse human over the last 20 year: A review towards lab on a chip devices, Micromachines. 13 187. (2022).
36. Efraín Polo-Cuadrado logoa, Osoriob, E. & Aldereteg, J. B. Karen Acosta-Quirogac, Paola Andrea Camargo-Ayalad, Iván Brito logoe, Jany Rodriguezf, Oscar Forero- Doriah, Edgard Fabián Blanco-Acuña, Margarita Gutiérrez, Nonlinear optical and spectroscopic properties, thermal analysis, and hemolytic capacity evaluation of quinoline-1,3-benzodioxole chalcone, RSC Adv. 14 10199–10208. (2024).
37. Ramalingam, S., Ebenezar, I. J. D. & Ramachandra Raja, C. Jobe Prabakar pectroscopic [IR and Raman] analysis and Gaussian hybrid computational investigation NMR, UV-Visible, MEP maps and Kubo gap on 2,4,6-nitrophenol. *J. Theor. Comput. Sci.* **1**, 1000108 (2014).

Acknowledgements

The authors extend their appreciation to the Ongoing Research, Funding program (ORF-2025-466), King Saud University, Riyadh, Saudi Arabia.

Author contributions

Conceptualization- K. Jayasheela, S. Murali Methodology- Mohammad Ahmad Wadaan, Nawaf D. Almoutiri, Madhappan Santhamoorthy, Saheed Olanrewaju Oseni Writing-review and Editing-S. Jeyaram, M. Vishalatchi and A.G. Bharathi Dileepan Supervision–S. Jeyaram.

Funding

"Ongoing Research, Funding program (ORF2025-466), King Saud University, Riyadh, Saudi Arabia".

Declarations

Competing interests

The authors declare no competing interests.

Additional information

Correspondence and requests for materials should be addressed to S.J.

Reprints and permissions information is available at www.nature.com/reprints.

Publisher's note Springer Nature remains neutral with regard to jurisdictional claims in published maps and institutional affiliations.